Kinetic and Equilibrium Study on Formic Acid Decomposition in Relation to the Water-Gas-Shift Reaction

Yoshiro Yasaka, Ken Yoshida, Chihiro Wakai, Nobuyuki Matubayasi, and Masaru Nakahara*

Institute for Chemical Research, Kyoto University, Uji, Kyoto 611-0011, Japan

Received: May 2, 2006; In Final Form: July 14, 2006

Kinetics and equilibrium are studied on the hydrothermal decarbonylation and decarboxylation of formic acid, the intermediate of the water-gas-shift (WGS) reaction, in hot water at temperatures of 170−330 °C, to understand and control the hydrothermal WGS reaction. ^{1}H and ^{13}C NMR spectroscopy is applied to analyze as a function of time the quenched reaction mixtures in both the liquid and gas phases. Only the decarbonylation is catalyzed by HCl, and the reaction is first-order with respect to both [H^+] and [HCOOH]. Consequently, the reaction without HCl is first and a half (1.5) order due to the unsuppressed ionization of formic acid. The HCl-accelerated decarbonylation path can thus be separated in time from the decarboxylation. The rate and equilibrium constants for the decarbonylation are determined separately by using the Henry constant (gas solubility data) for carbon monoxide in hot water. The rate constant for the decarbonylation is 1.5×10^{-5}, 2.0×10^{-4}, 3.7×10^{-3}, and 6.3×10^{-2} mol^{-1} kg s^{-1}, respectively, at 170, 200, 240, and 280 °C on the liquid branch of the saturation curve. The Arrhenius plot of the decarbonylation is linear and gives the activation energy as 146 ± 3 kJ mol^{-1}. The equilibrium constant K_{CO} = [CO]/[HCOOH] is 0.15, 0.33, 0.80, and 4.2, respectively, at 170, 200, 240, and 280 °C. The van't Hoff plot results in the enthalpy change of ΔH = 58 ± 6 kJ mol^{-1}. The decarboxylation rate is also measured at 240−330 °C in both acidic and basic conditions. The rate is weakly dependent on the solution pH and is of the order of 10^{-4} mol kg^{-1} s^{-1} at 330 °C. Furthermore, the equilibrium constant K_{CO2} = [CO_2][H_2]/[HCOOH] is estimated to be 1.0×10^2 mol kg^{-1} at 330 °C.

1. Introduction

In recent years,[1−6] formic acid has been found to decompose without catalysts in the following ways:

$$\mathrm{HCOOH} \rightleftarrows \mathrm{CO} + \mathrm{H_2O} \qquad \text{(decarbonylation)} \qquad (1)$$

$$\mathrm{HCOOH} \rightleftarrows \mathrm{CO_2} + \mathrm{H_2} \qquad \text{(decarboxylation)} \qquad (2)$$

The reversibility of the decarbonylation has been evidenced by the direct conversion of carbon monoxide to formic acid in hot water[7] and furthermore by the stability analysis based on the free energies for the species (HCOOH, CO, CO_2, H_2, and H_2O) involved in reactions 1 and 2.[8] The reversibility and the coupling of the reactions given by eqs 1 and 2 clearly indicate that formic acid exists as an intermediate in the water-gas-shift (WGS) reaction,[9−11] which has long been known to generate hydrogen from water as a clean fuel.[12] Now the WGS reaction is expressed as

$$\mathrm{CO} + \mathrm{H_2O} \rightleftarrows \mathrm{HCOOH} \rightleftarrows \mathrm{CO_2} + \mathrm{H_2} \qquad (3)$$

and the kinetics and equilibrium of the WGS reaction can be comprehensively established by examining the rate and equilibrium constants for the decarbonylation and the decarboxylation of formic acid. The kinetics and equilibrium study has been hampered by the following: (i) the reaction order of reaction 1 has not yet been established; (ii) these reactions can be catalyzed by metals used for reaction cells;[4,6,13] (iii) although the noncatalytic decarbonylation can be dominant in hot water, the reaction rate is very slow (a time scale of days to weeks below ~200 °C); and (iv) it is rather difficult to quantitatively analyze such main gaseous products as CO, CO_2, and H_2 in the heterogeneous system because of their distribution between the gas and liquid phases. In the present analysis, we decouple the two decomposition pathways of formic acid in eqs 1 and 2 by exploiting the catalytic effect of acid on the decarbonylation. The surface-catalytic effect is avoided by choosing quartz as a reactor material. HCl is employed for the time-scale separation of the relevant kinetic paths. All of the gaseous products are quantified in the sealed reactor by ^{1}H and ^{13}C NMR spectroscopy, and the carbon mass balance is confirmed.

Formic acid is involved as a key compound not only in the WGS reaction but also in a number of organic reactions recently revealed in hot water.[14,15] We need to establish the kinetics and mechanisms of the hydrothermal formation and decomposition reactions of formic acid, in view of the following three processes. (1) Formic acid, as an aldehyde (C1, single-carbon contained), is involved in the noncatalytic cross-disproportionations of aldehydes; an aldehyde is reduced to the corresponding alcohol and formic acid oxidized to carbonic acid or carbon dioxide.[14] (2) Formic acid reacts with formaldehyde (C1 aldehyde) in the presence of acid to form a C2 compound, glycolic acid, through the C−C bond formation as a chemical evolution process.[14] (3) Carbon monoxide, which is in hydrothermal equilibrium with formic acid, is released through the decarbonylation of aldehydes that can be generated by the heterolytic fragmentation of ethers.[15]

The decomposition of formic acid has been studied for more than a decade as previously referred to,[7] but its kinetics and equilibrium have not yet been established. Among the previous studies Bröll et al. reported the dominance of the decarbonyla-

* Corresponding author. E-mail: nakahara@scl.kyoto-u.ac.jp.

10.1021/jp0626768 CCC: $33.50
Published on Web 09/02/2006

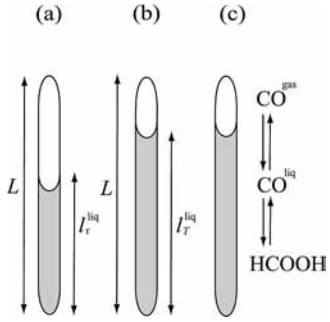

Figure 1. Definition of the filling factor of the sample at (a) room temperature ρ_r and (b) the reaction temperature ρ_T. The filling factor at the reaction temperature is larger than that at room temperature due to the decrease of water density at elevated temperature for $\rho_r > 0.33$. The expansion of the total length L of the quartz reactor is negligible in view of the thermal expansion coefficient of quartz. (c) Illustration of the dissolution equilibrium of CO in a sample.

tion path in the decomposition at low temperatures without kinetic analysis.[5] As for the decarboxylation, there are much more quantitative studies,[2−5,13] and the reaction rate has been obtained mainly under the surface catalytic effect of metals. Savage and co-workers studied the decomposition of formic acid in a flow reactor made of Hastelloy C-276 at 0.02 M (mol dm^{-3}) in the temperature range of 320−500 °C and showed that the main product was CO_2.[2] Other authors also reported at higher concentrations (0.13 and 1 M) that the decarboxylation is the main decomposition path.[3,4] McCollom et al. examined the decarboxylation of formic acid using a gold bag reactor with and without minerals and clarified that the catalytic effect is not given by minerals but by the transition metals except for gold.[13] They also observed the formation of formate ion from CO_2 and H_2 in basic conditions, which indicates the reversibility of the decarboxylation. Here we perform the detailed analysis of the decarbonylation and decarboxylation paths in noncatalytic quartz tube in a wide range of temperatures, concentrations, and pH values, with an attempt to establish the kinetics and equilibrium of the hydrothermal WGS reaction.

The experimental part is described in section 2. In section 3, results and discussion are given. In section 3.1, the reaction rate law of the decarbonylation is derived and its rate constant is determined. The equilibrium constant of the decarbonylation is determined in section 3.2. In section 3.3, the rate of the decarbonylation in the absence of strong acid is analyzed and the acid dissociation constant of formic acid is semiquantitatively estimated. The decarboxylation kinetics and equilibrium are in section 3.4. In section 3.5, a scheme to control the WGS reaction is presented. Conclusions are given in section 4.

2. Experimental Section

2.1. Materials and Apparatus. ^{13}C-enriched formic acid (99 atom % and 95% (w/w) in H_2O) and sodium formate (99 atom %) were obtained from ISOTEC and used as received. Aqueous solutions of HCl (0.01, 0.02, 0.05, 0.1, and 1.0 M) were obtained from Nacalai. A reactor was made of a sealed quartz tube of 1.5 mm i.d. and 3.0 mm o.d. and 10−20 cm long. As shown in Figure 1, the reaction solution was introduced to occupy a specified portion (controlled with an accuracy of 1%) of the tube reactor. The volume (length, l_T^{liq}) ratio of the liquid phase to the total (L) is hereafter denoted as the filling factor:

$$\rho_T = \frac{\text{the volume of the liquid phase}}{\text{the total volume of the reactor}} = \frac{l_T^{liq}}{L} \qquad (4)$$

where the subscript T represents the temperature. Note that the filling factor ρ_T at a reaction temperature T is larger than that at room temperature 30 °C, ρ_r, due to the expansion of water when $\rho_r > 0.33$ (at densities higher than the critical density of water); compare Figure 1a and Figure 1b. The gaseous reaction product is in dissolution equilibrium at each temperature (Figure 1c). The value of ρ_T can be calculated from ρ_r by using the tabulated density of water along the saturation curve.[16]

Each sample was heated for a specified reaction time in a programmable electric furnace kept at the reaction temperature (170−330 °C) with an accuracy of 1 °C. At the reaction temperature, the liquid and gas phases coexist and the reaction proceeds in the liquid phase. After the sample was quenched by air, ^1H and ^1H-decoupled ^{13}C NMR spectra were observed at 30 °C with a NMR spectrometer (JEOL ECA400, magnetic field strength of 9.4 T). Such gaseous products as CO, CO_2, and H_2 coexist in the liquid and gas phases, and the NMR spectra were measured for each phase by the method described elsewhere.[15] The spectral measurements were carried out as a function of reaction time to examine the time evolution of the reactant and products.

2.2. Yield Analysis. The concentration of formic acid [HCOOH] was estimated by the ^1H peak intensity relative to that of solvent H_2O (55.5 M) in the liquid phase. The fraction of residual formic acid, denoted as x_{HCOOH}, is expressed by

$$x_{HCOOH} = \frac{[HCOOH]}{[HCOOH]_0} \qquad (5)$$

where $[HCOOH]_0$ is the initial concentration of formic acid. To determine the yields of gaseous products, CO, CO_2, and H_2, we measured their concentrations in both the liquid and gas phases. The concentration of CO or CO_2 dissolved in water was evaluated by the liquid-phase ^{13}C spectrum using HCOOH as the internal reference; [HCOOH] was determined in advance by the ^1H spectrum. For the gas-phase ^{13}C spectrum, HCOOH in the liquid phase of the same sample was used as the external reference to quantify the gas-phase concentration of CO or CO_2. Thus the total yield of CO, expressed as x_{CO}, is calculated by

$$x_{CO} = \frac{[CO]^{liq} + [CO]^{gas}\dfrac{1-\rho_r}{\rho_r}}{[HCOOH]_0} \qquad (6)$$

Here, $[CO]^{liq}$ and $[CO]^{gas}$ are the concentrations of CO in the liquid and gas phases, respectively, obtained at 30 °C, and the subscript r indicates the temperature (30 °C) at which the NMR analysis is performed. The coefficient $(1 - \rho_r)/\rho_r$ (the volume ratio of the gas to the liquid phase) is the conversion factor for the gas-phase concentration to that in the liquid phase. The same procedure was used for CO_2. It was found that the carbon mass balance was maintained during the reaction within 10%. The source of error is the absence of an internal reference in the estimate of the gaseous products and the magnetization transfer from proton to carbon through the C−H bond of formic acid when the ^1H-decoupled ^{13}C spectrum is taken.[17] The maintained mass balance indicates that CO and CO_2 do not leak through the reactor walls. The yield of H_2 was estimated by the gas-phase ^1H spectrum using solvent H_2O of the same sample as the external reference. The concentration of dissolved H_2 was not incorporated into the yield, since it is not measurable by the interference of the strong solvent peak. This may lead to an underestimate of the yield by ~5%. In addition, the smallest molecule H_2 escapes out of the quartz reactor with a time scale

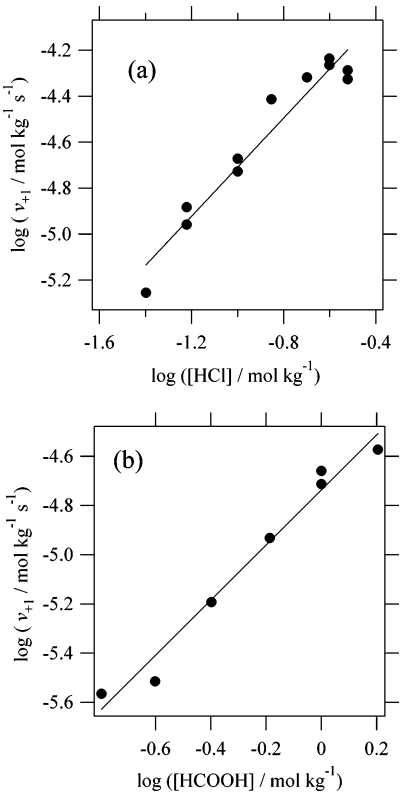

Figure 2. (a) The logarithm−logarithm plot of the initial rate v_{+1} of the decarbonylation against [HCl] at the formic acid initial concentration $[HCOOH]_0 = 1.0$ mol kg^{-1} and the reaction temperature of 200 °C. The line is the linear fit of the experimental data, and its slope is 1.1 ± 0.1. (b) The logarithm−logarithm plot of the initial rate v_{+1} of the decarbonylation against $[HCOOH]_0$ at [HCl] = 0.10 mol kg^{-1} and 200 °C. The line is the linear fit of the experimental data, and its slope is 1.1 ± 0.1.

of ∼100 h. Thus the yield of H_2 was estimated only in the study of the decarboxylation at 330 °C, in which the reaction time scale is ∼10 h.

In the determination of the equilibrium constants of the decarbonylation and the decarboxylation, the liquid-phase concentration (in situ concentration) of each gaseous product at the reaction temperature is required. The yields previously obtained can be converted into in situ concentrations by taking into account the dissolution equilibrium of the gases at the reaction temperature (the procedure is described in section 3.2). For this purpose, the liquid−gas distribution constants (Henry constants) of CO, CO_2, and H_2 at elevated temperatures were taken from ref 18.

3. Results and Discussion

3.1. Decarbonylation Kinetics. We can study the rate law for the decarbonylation by investigating the initial rate in the presence of HCl. When the HCl concentration is larger than 2.0×10^{-2} mol kg^{-1}, the decarbonylation is more than 50 times faster than the decarboxylation and can be separately quantified. When the decarboxylation can be neglected, the initial rate of formic acid decomposition is given by

$$v_{+1} = -\left.\frac{\mathrm{d[HCOOH]}}{\mathrm{d}t}\right|_0 = k_{+1}[\mathrm{H^+}]^a[\mathrm{HCOOH}]_0^{\,b} \qquad (7)$$

Here v_{+1} is the reaction velocity, k_{+1} is the rate constant, $[HCOOH]_0$ is the initial concentration of formic acid, and the parameters a and b are the reaction orders with respect to the proton (HCl) and formic acid, respectively.

TABLE 1: The Rate Constant k_{+1} and the Equilibrium Constant K_{CO} for the Decarbonylation, and the Acid Dissociation Constant K_a of Formic Acid in the Temperature Range of 170−300 °C on the Liquid Branch of the Saturation Curve

T/°C	$\log(k_{+1}/\mathrm{mol^{-1}\ kg\ s^{-1}})$	K_{CO}	pK_a
170	−4.82	0.15	
185	−4.22		
200	−3.71	0.33	4.2
210	−3.29	0.44	3.8
220	−2.98		3.8
230	−2.75		4.0
240	−2.43	0.80	4.2
250		1.2	4.6
260	−1.91		4.6
280	−1.20	4.2	4.9
300			5.0

First, we determine a by measuring v_{+1} with various HCl concentrations at $[HCOOH]_0 = 1.0$ mol kg^{-1} and the temperature of 200 °C on the liquid branch of the saturation curve. The logarithm of the initial reaction rate is plotted against the logarithm of the HCl concentration in Figure 2a. The plot is fitted well to a straight line with a slope of 1.1 ± 0.1. Hence, we can regard the order a as 1. Second, in order to determine the order b, we have observed v_{+1} by varying the initial formic acid concentration at [HCl] = 0.10 mol kg^{-1} and the temperature of 200 °C. The logarithm of the initial reaction rate is plotted against the logarithm of the formic acid concentration in Figure 2b. The slope of the linear fitting line is 1.1 ± 0.1. In consequence, the decarbonylation follows the simple second-order rate law as

$$v_{+1} = k_{+1}[\mathrm{H^+}][\mathrm{HCOOH}] \qquad (8)$$

The rate law thus established has been further confirmed by studying the decomposition of HCOONa that hydrolyzes to generate a basic condition. In this case, the amount of CO produced from HCOONa was below the detection limit.[19]

We determined the second-order rate constant k_{+1} in the temperature range of 170−280 °C on the liquid branch of the saturation curve. The results are shown in Table 1 and plotted against the reciprocal temperature in Figure 3. The Arrhenius plot is linear, and the activation energy for the decarbonylation is evaluated to be as high as 146 ± 3 kJ mol^{-1}. For the decarbonylation mechanism, we may consider the following:

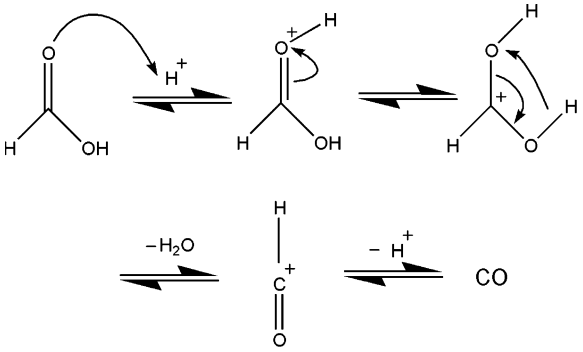

(9)

First, formic acid is protonated on the oxygen atom of the carbonyl group (the protonation may proceed on the hydroxyl group); second, it is dehydrated to form the protonated carbon monoxide; and finally it releases the proton. The first and third steps are fast, and the second is the rate-determining step.

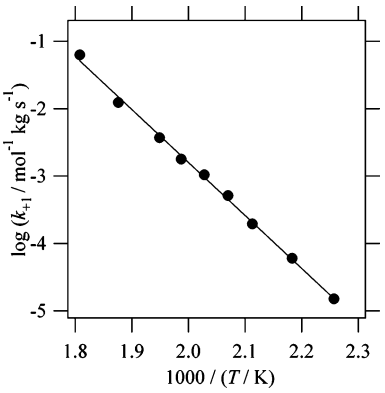

Figure 3. The Arrhenius plot of the rate constant k_{+1} of the decarbonylation. The line is the linear fit of the experimental data. The slope of the line gives the activation energy of the decarbonyaltion: $E_a = 146 \pm 3$ kJ mol^{-1}.

It is of interest to compare our result with a previous one performed without water (in neat conditions). The reaction was studied in the gas phase by Blake et al.,[20] and an activation energy of 119 kJ mol^{-1} was reported at ~500 °C. The activation energy of the hydrothermal reaction is not smaller but larger than that of the neat gas-phase one. In the hydrothermal conditions, a heterolytic bond-breakage process leading to an ionic transition state is more probable because the high polarity of the solvent can stabilize ionic states and the ionic species are involved in the hydrothermal process as shown by the scheme in eq 9. In the gas-phase decarbonylation, on the other hand, a homolytic bond-breakage process and a neutral transition state are assumed.[20] Any difference in the transition state as well as the extent of stabilization of relevant species by solvation and protonation can account for the difference in the activation energy (and free energy) between the liquid- and gas-phase reactions. It is desirable to perform a quantum-chemical calculation for the acid-catalyzed decarbonylation to get insight in the transition-state structure for the hydrothermal reaction.[11,21−23]

3.2. Decarbonylation Equilibrium. In this section we determine the equilibrium constant of the decarbonylation of formic acid in hot water in the temperature range of 170−280 °C. By adding such a strong acid as HCl, we can separate the time scale of the decarbonylation from that of the decarboxylation. As can be seen in Figure 4a and Figure 4b, the decarbonylation is accelerated by a factor of ~10 in the presence of HCl at 0.10 mol kg^{-1}. In the absence of HCl, it takes several tens of hours for the decarbonylation equilibrium to be attained and the nonnegligible amount of CO_2 is produced in competition with the decarbonylation.

The equilibrium constant of the decarbonylation in hot water is defined as

$$K_{CO} = \left.\frac{[CO]^{liq}}{[HCOOH]^{liq}}\right|_{eq} \tag{10}$$

where the symbol $|_{eq}$ represents the value evaluated at equilibrium, and water as a reactant species is not contained since it is present in excess as a solvent. What is directly obtainable from the yield analysis (see eqs 5 and 6) is not K_{CO} but a quantity denoted as the decarbonylation quotient Q_{CO}:

$$Q_{CO} = \left.\frac{x_{CO}}{x_{HCOOH}}\right|_{eq} \tag{11}$$

where x_{HCOOH} and x_{CO} are provided by eqs 5 and 6, respectively.

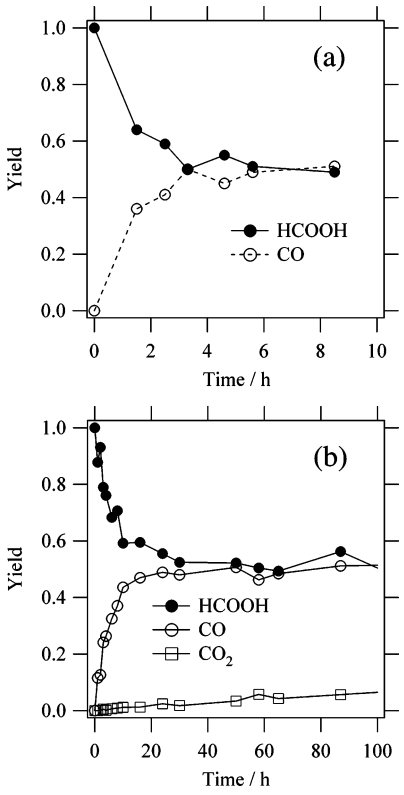

Figure 4. The time evolution of formic acid decomposition (a) with and (b) without HCl at 250 °C. The initial compositions are (a) 0.16 mol kg^{-1} for formic acid with HCl at 0.10 mol kg^{-1} and (b) 1.0 mol kg^{-1} for formic acid without HCl. In panel a, the plotted yield of CO is calculated as $1 - x_{HCOOH}$.

As the reaction takes place in the subcritical water along the saturation curve, not all of the CO produced by the decarbonylation remains in the liquid phase, but a considerable amount of CO is accommodated in the gas phase of the sample. Hence Q_{CO} is larger than K_{CO}. To determine K_{CO} we need to calculate the fraction, β, of CO distributed in the liquid phase.

$$\beta = \frac{\text{moles of CO in the liquid phase}}{\text{total moles of CO}} \tag{12}$$

Then the relation of Q_{CO} and K_{CO} is written as

$$K_{CO} = \frac{\beta x_{CO}}{x_{HCOOH}} = \beta Q_{CO} \tag{13}$$

where formic acid is considered to be present only in the liquid phase.

The value of β is dependent on the solubility (Henry constant) of CO at the reaction temperature and the filling factor defined by eq 4. To evaluate the value of β, we assume the following: (1) The dissolution of the gases is sufficiently faster than the decarbonylation and the decarboxylation. (2) The Henry law holds for the dissolution of CO into hot water. (3) The equation of state for the ideal gas holds for CO in the gas phase. The Henry constant k_H is the mole ratio of liquid H_2O to CO dissolved in hot water which is in dissolution equilibrium with hypothetical ideal gas of CO at 1 MPa.

When the partial pressure of CO is given by p_{CO}/MPa, we have the molar (volume) concentration of dissolved CO as

$$[CO]^{liq} = \frac{p_{CO} d_T}{k_H} \tag{14}$$

where d_T is the molar concentration of liquid water at the reaction temperature T on the saturation curve. The gas-phase molar concentration of CO is expressed by

$$[\mathrm{CO}]^{\mathrm{gas}} = \frac{p_{\mathrm{CO}}}{RT} \tag{15}$$

according to the ideal gas law; R is the gas constant. Using eqs 10−15, we can evaluate the value of β as

$$\beta = \frac{[\mathrm{CO}]^{\mathrm{liq}}\rho_T}{[\mathrm{CO}]^{\mathrm{liq}}\rho_T + [\mathrm{CO}]^{\mathrm{gas}}(1-\rho_T)} = \frac{\rho_T}{K_{\mathrm{D}}(\mathrm{CO})(1-\rho_T)+\rho_T} \tag{16}$$

where the liquid−gas distribution constant is introduced by

$$K_{\mathrm{D}}(\mathrm{CO}) = \frac{k_{\mathrm{H}}}{RTd_T} = \frac{[\mathrm{CO}]^{\mathrm{gas}}}{[\mathrm{CO}]^{\mathrm{liq}}} \tag{17}$$

and ρ_T is the filling factor at the reaction temperature. The Henry constant k_{H} taken from ref 18 and the molar concentration d_T of pure water tabulated in ref 16 are used to evaluate $K_{\mathrm{D}}(\mathrm{CO})$. As the temperature increases along the saturation curve, liquid water is expanded and CO becomes more soluble in water in the temperature range studied here; $K_{\mathrm{D}}(\mathrm{CO}) = 29.6$, 13.8, and 8.4 at 170, 240, and 280 °C, respectively. The value of ln K_{D}(CO) and its temperature dependence are in good agreement with those in a previous computational study.[8] Now the equilibrium constant K_{CO} is explicitly written in terms of the directly measurable quantities Q_{CO} and ρ_T as

$$K_{\mathrm{CO}} = \frac{\rho_T}{K_{\mathrm{D}}(\mathrm{CO})(1-\rho_T)+\rho_T} Q_{\mathrm{CO}} \tag{18}$$

On the basis of this equation, we can determine K_{CO} by measuring the equilibrium mole fraction $x_{\mathrm{HCOOH}}^{(\mathrm{eq})}$ of formic acid under a given filling factor ρ_T. We can evaluate Q_{CO} in eq 18 from eq 11; $x_{\mathrm{CO}}^{(\mathrm{eq})} = 1 - x_{\mathrm{HCOOH}}^{(\mathrm{eq})}$. Values of the equilibrium constant K_{CO} as the average of two measurements (13 measurements for 240 °C) of different filling factors are listed in Table 1 at 170−280 °C.

Equation 18 is also viewed as an expression for the variation of $x_{\mathrm{HCOOH}}^{(\mathrm{eq})}$ with the filling factor ρ_T. Solving eqs 11 and 18 with respect to $x_{\mathrm{HCOOH}}^{(\mathrm{eq})}$, we obtain

$$x_{\mathrm{HCOOH}}^{(\mathrm{eq})} = \frac{1}{K_{\mathrm{CO}} + 1 - K_{\mathrm{CO}}K_{\mathrm{D}}(\mathrm{CO}) + \dfrac{K_{\mathrm{CO}}K_{\mathrm{D}}(\mathrm{CO})}{\rho_T}} \tag{19}$$

The equilibrium fraction $x_{\mathrm{HCOOH}}^{(\mathrm{eq})}$ is a monotonically increasing function of ρ_T. When the filling factor is small (a small fraction of the reactor volume is occupied by the reaction solution), the equilibrium apparently favors the CO side of eq 11. This is because the CO produced by the decarbonylation escapes into the gas phase and induces further decomposition of formic acid. When ρ_T approaches the maximum value of 1 (fully filled), the equilibrium fraction steeply rises to the limiting value of $1/(K_{\mathrm{CO}} + 1)$, resulting in $Q_{\mathrm{CO}} = K_{\mathrm{CO}}$. Note that eq 19 holds only when the reaction solution is so dilute that the assumptions for the formulation of eqs 14 and 15 are valid.

The equilibrium fraction $x_{\mathrm{HCOOH}}^{(\mathrm{eq})}$ of formic acid is plotted against ρ_T at 240 °C in Figure 5. There are included results for

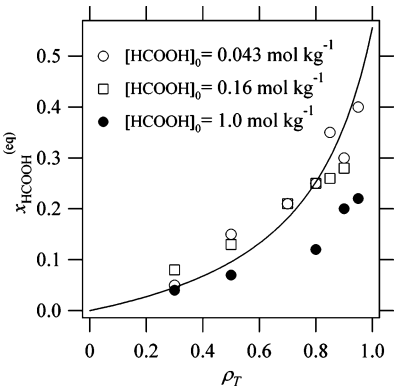

Figure 5. The observed equilibrium yield $x_{\mathrm{HCOOH}}^{(\mathrm{eq})}$ of formic acid against the filling factors ρ_T at 240 °C. Open circles correspond to the initial composition of 0.043 mol kg^{-1} for formic acid with HCl at 0.040 mol kg^{-1}, open squares to 0.16 mol kg^{-1} for formic acid with HCl at 0.10 mol kg^{-1}, and filled circles to 1.0 mol kg^{-1} for formic acid with HCl at 0.10 mol kg^{-1}. The equilibrium yield of formic acid calculated by eq 19 with $K_{\mathrm{CO}} = 0.8$ is shown by the solid line.

different initial concentrations of formic acid, 0.040, 0.16, and 1.0 mol kg^{-1}, and for each concentration the monotonic increase of $x_{\mathrm{HCOOH}}^{(\mathrm{eq})}$ with ρ_T is evident. For the initial concentrations of 0.040 and 0.16 mol kg^{-1}, the results are fitted well to eq 19 using the value of K_{CO} in Table 1. The good fit indicates that eq 19 represents well how the phase distribution of CO affects the decarbonylation equilibrium. When the initial concentration is increased to such a high value as 1.0 mol kg^{-1}, the equilibrium concentration of formic acid is considerably lower than that expected with $K_{\mathrm{CO}} = 0.8$ at a high filling factor $\rho_T > 0.8$; see Figure 5. One may consider the high pressure of CO gas as one of the reasons for the low $x_{\mathrm{HCOOH}}^{(\mathrm{eq})}$. The CO pressure is estimated as 20, 10, and 3 MPa, however, for $\rho_T = 0.95$, 0.80, and 0.50. According to the Redlich−Kwong equation of state,[24] the corresponding fugacity coefficient is not far from 1. Thus the deviation from the ideal-gas approximation does not account for the small $x_{\mathrm{HCOOH}}^{(\mathrm{eq})}$. Another reason can be considered as described below. It has been often observed that formic acid decomposes beyond the equilibrium limit (chemical-potential crossover) and then very slowly recovers through the backward reaction involving the liquid−gas distribution of CO; thus the formic acid concentration oscillates. The oscillation is more likely to occur when the initial concentration of formic acid is as high as 1.0 mol kg^{-1} and at the same time HCl accelerates the decarbonylation. Probably the oscillation is caused from the delay of the dissolution of CO against the decarbonylation (the assumption of the fast equilibrium of the dissolution is not valid). When the oscillation takes place, a longer time is required for the system to attain the true equilibrium state, making an accurate determination of $x_{\mathrm{HCOOH}}^{(\mathrm{eq})}$ almost impossible. The equilibrium constant K_{CO} was successfully determined at such dilute formic acid concentrations as 0.04 and 0.16 mol kg^{-1}.

The equilibrium constants K_{CO} at 170−280 °C are listed in Table 1, and the van't Hoff plot of the decarbonylation is shown in Figure 6. The enthalpy change of the decarbonylation ΔH_{CO} may be defined along the saturation curve as

$$\Delta H_{\mathrm{CO}} = -R\frac{\partial \ln(K_{\mathrm{CO}}[\mathrm{H_2O}])}{\partial(1/T)} = -R\left(\frac{\partial \ln K_{\mathrm{CO}}}{\partial(1/T)} + \frac{\partial \ln [\mathrm{H_2O}]}{\partial(1/T)}\right) \tag{20}$$

Here, the partial differentiation is done along the saturation curve instead of constant pressure. According to the van't Hoff plot and the equation of state for water, ΔH_{CO} is obtained as 58

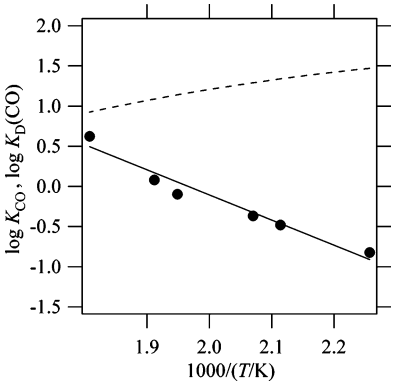

Figure 6. The van't Hoff plots of the equilibrium constants K_{CO} and K_D(CO). The filled circles indicate K_{CO}, and they are fitted to the solid line. The slop of the solid line gives the enthalpy change of the decarbonylation $\Delta H = 58 \pm 6$ kJ mol^{-1}. The dashed line represents K_D(CO) taken from ref 15.

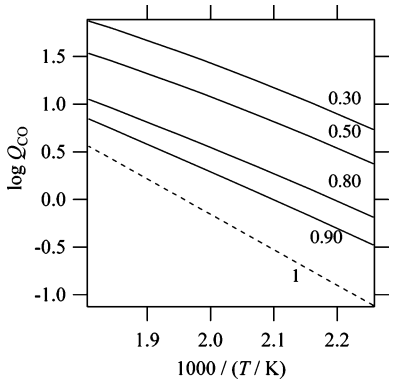

Figure 7. The temperature dependence of Q_{CO}. Each of the contours corresponds to a fixed filling factor ρ_T indicated in the figure. The dashed line corresponds to the filling factor of 1 (totally filled), where $Q_{CO} = K_{CO}$.

$\pm$ 6 kJ/mol. Using the heat of formation and the heat capacity of gaseous CO, CO_2, and H_2O,[25,26] the enthalpy change for the gas-phase reaction is 28 kJ mol^{-1} at 250 °C. This means that the enthalpy difference between the initial (HCOOH) and the final (CO + H_2O) states is increased by ~30 kJ mol^{-1} due to the solvation of each species and the condensation of water. The dissolution heat of gaseous formic acid is expected to be considerably larger than the condensation heat of water (45 kJ mol^{-1} at 30 °C). Matubayasi et al. calculated the free energies of the formic acid and carbon monoxide in hot water and derived the equilibrium constant of the decarbonylation at 25−400 °C.[8] The enthalpy change obtained by the temperature differentiation of the equilibrium constant is somewhat smaller ($\Delta H_{CO} = 23$ kJ mol^{-1}) than the experimental one. This magnitude of discrepancy is reasonable as the calculated values of the standard free energy of reaction differ by ~2 kcal mol^{-1}.

We have determined K_{CO} and discussed the thermodynamic property of the decarbonylation. On the other hand, the decarbonylation quotient Q_{CO} is more useful for practical use, since it is directly related to the product yield as eq 11. Now we can demonstrate how the decarbonylation quotient Q_{CO} is controlled by the temperature and the filling factor by using K_{CO} obtained above from eq 18. The result is plotted against the temperature in Figure 7 for $\rho_T = 0.30$, 0.50, 0.80, 0.90, and 1. When the filling factor is lowered, the equilibrium shifts to the CO side; a large portion of the CO produced by the decarbonylation is accommodated not in the liquid phase but in the gas phase.

The difference between K_{CO} and Q_{CO} is also striking in their temperature dependence. As the temperature dependence of K_{CO} is expressed by the enthalpy change ΔH_{CO}, we define the corresponding quantity for Q_{CO} as

$$\Delta H'_{CO} = -R\frac{\partial \ln(Q_{CO}[H_2O])}{\partial(1/T)} \tag{21}$$

where again the partial differentiation is along the saturation curve. By virtue of eqs 18 and 20, it follows that

$$\Delta H'_{CO} = \Delta H_{CO} - R\frac{1}{1+\dfrac{\rho_T}{K_D(CO)(1-\rho_T)}}\frac{\partial \ln K_D(CO)}{\partial(1/T)} = \Delta H_{CO} + \frac{1}{1+\dfrac{\rho_T}{K_D(CO)(1-\rho_T)}}\Delta H_D \tag{22}$$

where the value of ρ_T is fixed and ΔH_D is the dissolution enthalpy of CO. $K_D(CO) = 8.4$ at 280 °C and is larger at lower temperatures. In this case, the coefficient of ΔH_D in eq 22 is approximately unity except for a very high filling factor, thus we have $\Delta H'_{CO} = \Delta H_{CO} + \Delta H_D$ and $\Delta H_D = -24$ kJ mol^{-1}. Therefore, the apparent enthalpy change of the decarbonylation is ~40% smaller in magnitude than the thermodynamic one due to the coupling of the dissolution equilibrium heat of CO. It should be noted that the product yields of such a reaction in subcritical water are modified by the liquid−gas distribution of gases.

3.3. Decarbonylation Kinetics without HCl. In the absence of strong acid, the decarbonylation is considered to be driven by the proton dissociated from formic acid.[23] The acid dissociation constant of formic acid, K_a, leads to the expression for the proton concentration in formic acid solution as

$$[H^+] = \sqrt{[HCOOH]K_a} \tag{23}$$

Here we have neglected the activity coefficients for the ions. Combining eqs 8 and 23, we have the decarbonylation rate in the absence of strong acid as follows:

$$-\frac{d[HCOOH]}{dt} = k_{+1}\sqrt{K_a}[HCOOH]^{1.5} \tag{24}$$

It is important to confirm the reaction order 1.5 that comes from the second-order rate expression given by eq 8. The formic acid concentration was varied over a wide range of 0.44−2.9 mol kg^{-1} at 240 °C. The filling factor ρ_r was sufficiently small (0.50) so that the backward reaction may be neglected. We have plotted the logarithm of the initial rate of the decrease of formic acid against the logarithm of the initial concentration of formic acid (Figure 8). The experimental results are fitted to a straight line, and its slope gives the rate order with respect to formic acid as 1.6 $\pm$ 0.1. This is consistent with the expression of eq 24, supporting the validity of eq 8. The dependence of the reaction rate on the concentration of formic acid is larger in the absence of HCl than that in the presence.

In the absence of HCl, the apparent rate constant $k_{+1}(K_a)^{1/2}$ of eq 24 allows us to approximately evaluate the pK_a of formic acid by the reaction-rate measurement; note that the value of k_{+1} is already determined in section 3.1. The values of pK_a are listed in Table 1 in the temperature range of 200−300 °C along the liquid branch of the saturation curve. The pK_a value at

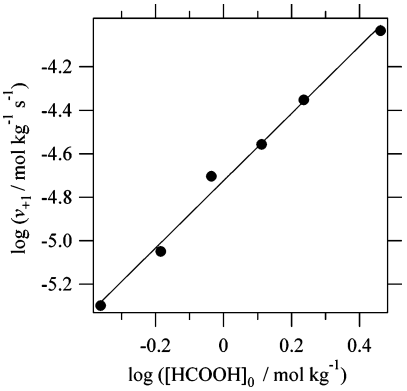

Figure 8. The logarithm−logarithm plot of the initial rate v_{+1} of the decarbonylation at 240 °C against the initial formic acid concentration $[HCOOH]_0$. The solid line is the linear fit of the experimental data, and its slope is 1.6 ± 0.1.

200 °C (4.2) is similar to that at 30 °C (pK_a = 3.75).[27] As the temperature rises to 300 °C, the acidity of formic acid decreases by a factor of 10. The decrease of the acidity between 200 and 300 °C is qualitatively in agreement with the behavior of the dielectric constant ϵ_r; ϵ_r = 35 and 20 at 200 and 300 °C, respectively. Between room temperature and 200 °C, pK_a seems to change weakly with temperature. This indicates the compensation of the decrease in solvation energy and the increase in the entropy term with increasing temperature from 30 to 200 °C. It is known that the dissociation of formic acid is weakly dependent on the temperatures in ambient conditions. According to the precise electrochemical measurements, pK_a varies only by 0.06 pK_a unit in the temperature range of 0−60 °C with a shallow minimum at around 25 °C.[27]

3.4. Decarboxylation Kinetics and Equilibrium. Now we proceed to the kinetic study of the decarboxylation. In the decomposition of sodium formate in hot water, the decarboxylation is the dominant pathway as shown in Figure 9a. This indicates that the ionic species $HCOO^-$ is involved in the decarboxylation,[28] and the following simple rate law is expected:

$$\frac{d[CO_2]}{dt} = v_{+2} = k[HCOO^-] \qquad (25)$$

However, eq 25 is found to contradict the decarboxylation rate of formic acid in the presence of HCl. In such acidic conditions, where a small fraction of formic acid dissociates to $HCOO^-$, the decarboxylation rate is observed to be still of the same order of magnitude with that of sodium formate in aqueous solution; compare Figure 9a and Figure 9b. The weak pH dependence of the decarboxylation rate can be explained in the following way. We assume that the decarboxylation through $HCOO^-$ is induced by both the acid and the neutral water molecule. Thus the rate law is written as

$$v_{+2} = k_{acid}[H^+][HCOO^-] + k_{water}[HCOO^-] \qquad (26)$$

where k_{acid} and k_{water} are, respectively, the rate constants for the acid-induced and water-induced decarboxylation. The reactivity of the neutral water molecule is revealed by kinetic studies on recently found hydrothermal reactions.[14] In order to clarify the pH dependence of the decarboxylation rate given by eq 26, it is useful to rewrite eq 26 as

$$v_{+2} = k_{acid}K_a[HCOOH] + k_{water}[HCOO^-] = k_{acid}K_a c_T(1-\alpha) + k_{water}c_T\alpha \qquad (27)$$

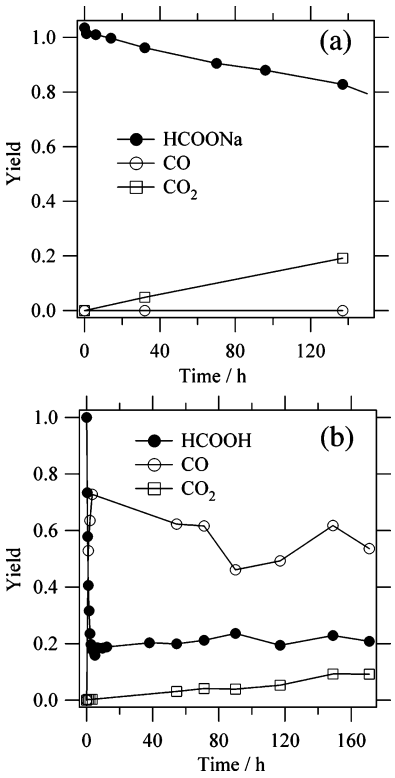

Figure 9. The time evolution of the reactant and product yields for the decomposition at 240 °C and ρ_T = 0.95 of (a) HCOONa at 1.0 mol kg^{-1} and (b) HCOOH at 1.0 mol kg^{-1} with HCl at 0.10 mol kg^{-1}.

where K_a is the acid dissociation constant of formic acid, c_T = [HCOOH] + [$HCOO^-$], the stoichiometric concentration of formic acid, and α = [$HCOO^-$]/c_T, the degree of dissociation of formic acid. The first term is important in strongly acidic conditions where the acid dissociation of formic acid is suppressed; $v_{+2} \rightarrow k_{acid}K_a c_T$ as $\alpha \rightarrow 0$. The second term, in turn, is important for the reaction of sodium formate where $\alpha \approx 1$.The rate law (eq 27) predicts that the decarboxylation rate is independent of the concentration of HCl added to formic acid; formic acid is a weak acid and its dissociation is negligible in the presence of HCl. This is indeed what is observed experimentally; the decarboxylation rate of formic acid at 1.0 mol kg^{-1} with HCl at 0.080 mol kg^{-1} was equal (within the experimental error) to that of formic acid at 1.0 mol kg^{-1} with HCl at 0.020 mol kg^{-1}.

Maiella et al.[4] performed kinetic analysis of the decarboxylation based on a different reaction mechanism. They assumed that the species HCOOH and $HCOO^-$ simultaneously decarboxylate with respective rate constants, and the total decarboxylation rate is given by the sum. McCollom et al. also adopted this assumption.[13] The rate law derived is coincident in form to eq 27 despite the difference in the reaction mechanism. It is therefore of interest to do a computational study on the transition state for distinguishing the reaction mechanism.[28]

The rate constants $k_{acid}K_a$ and k_{water} are determined, respectively, by measuring the decarboxylation rate in strongly acidic and basic conditions, according to eq 27. The results obtained are summarized in Table 2. The precision of the rate constant is relatively low (∼10%) because the ^{13}C NMR measurement lacks an internal reference. In addition, the surface of the quartz tube is corroded in basic conditions and the reaction analysis can be carried out only at an early stage. Two rate constants $k_{acid}K_a$ and k_{water} are of the same order. This indicates that the decarboxylation rate changes only weakly with pH in contrast to the decarbonylation. The magnitude relation between $k_{acid}K_a$

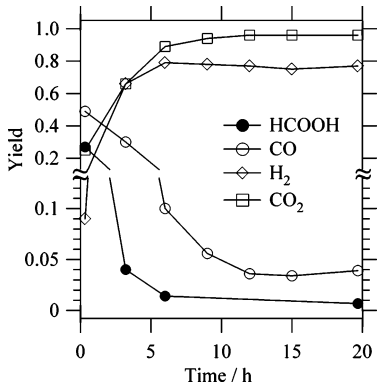

Figure 10. The time evolution of the reactant and product yields for the decomposition of 1.0 mol kg^{-1} formic acid at 330 °C and $\rho_T \approx 0.99$ (the volume of the gas phase is negligible). The temperature is too high to follow the decarbonylation kinetics. Note that the graduation of the ordinate is changed at 0.13.

TABLE 2: The Rate Constants $k_{acid}K_a$ and k_{water} in the Temperature Range of 200−330 °C on the Liquid Branch of the Saturation Curve

T/°C	$\log(k_{acid}K_a/s^{-1})$	$\log(k_{water}/s^{-1})$
200	−6.6	
230	−5.7	
240	−6.1	−6.4
260	−5.9	−5.5
280	−5.4	−4.9
300	−4.6	−4.3
330	−4.1	−3.4

and k_{water} changes at ∼280 °C, and at the higher temperature of ∼330 °C, k_{water} overwhelms $k_{acid}K_a$. The smaller temperature dependence of $k_{acid}K_a$ than that of k_{water} can result from the decrease of K_a with temperature (Table 1). Taking advantage of the different pH dependence of the decarbonylation and decarboxylation rates, the path control of the hydrothermal decomposition of formic acid can be realized. The decarbonylation is the major path in acidic conditions due to the catalytic effect of the proton, while the decarboxylation becomes dominant when pH > 4.

Here we mention the decarboxylation equilibrium. We have followed the decarboxylation for a sufficiently long time and showed the time evolution of products at 330 °C as in Figure 10. As can be seen, the fast decarbonylation attains the equilibrium within an hour, and this preequilibrium is maintained ($x_{CO}/x_{HCOOH} \sim 5$) during the course of the slow decarboxylation. The parallel decrease of formic acid and carbon monoxide almost stops at ∼20 h, and this indicates that the decarboxylation equilibrium is attained. The equilibrium yield of each component is 0.96, 0.78, 0.04, and 0.007 for CO_2, H_2, CO, and HCOOH, respectively. The yield of hydrogen is too small compared with that of CO_2, and it is due to the leakage of hydrogen through the reactor walls (the time scale of the leakage is estimated to be ∼100 h from long-time experiments). The equilibrium constant of the decarboxylation is defined by

$$K_{CO2} = \left.\frac{[CO_2]^{liq}[H_2]^{liq}}{[HCOOH]^{liq}}\right|_{eq} \tag{28}$$

By taking account of the liquid−gas distribution of H_2 and CO_2 in the same way as that described in section 3.2, the value of K_{CO2} at 330 °C is estimated to be 1×10^2 mol kg^{-1}. Our result shows that the decarboxylation equilibrium strongly favors the CO_2 side, and this is consistent with the thermodynamic calculations by McCollom et al.[13] and statistical−mechanical calculations.[8]

3.5. Control of Water-Gas-Shift Reaction. In the previous sections, we have established the kinetics and equilibrium of the decarbonylation and the decarboxylation of formic acid which constitute the hydrothermal water-gas-shift (WGS) reaction. Based on the above analysis, here we propose a scheme for controlling the WGS reaction for hydrogen storage in the form of formic acid.

The most important feature of the hydrothermal WGS reaction is the existence of the intermediate, formic acid. When the time scales of the decarbonylation and the decarboxylation are separated, the WGS reaction can be regarded as a stepwise reaction and it is possible to isolate the intermediate (formic acid) from the reaction mixture before the second slow step initiates. In the presence of HCl, the decarbonylation has a much shorter time scale than does the decarboxylation. In this case, the process for hydrogen production from carbon monoxide can be divided into two parts: the production of formic acid which can be used as a compact and handy hydrogen source, and the hydrogen supply from formic acid when hydrogen energy is needed. The first part is the reverse decarbonylation, and the second is the decarboxylation. The conversion ratio of the former process (formic acid production) is governed by the quotient Q_{CO} mentioned in section 3.3, and more formic acid is yielded (small Q_{CO}) at a lower temperature and/or a higher filling factor, as seen from Figure 7. For the latter process (the decarboxylation of formic acid), the equilibrium constant K_{CO2} is relatively large (∼100 at 330 °C) and formic acid can be converted into $CO_2 + H_2$ almost completely. The hydrogen-generating process should be carried out in weakly acidic conditions so that the decarboxylation may be the main decomposition path of formic acid. Basic conditions are, however, not appropriate, because basic conditions will stabilize the reactant (formic acid) in the form of the formate anion; formic acid is by far a stronger acid than CO_2. In addition, to run the reaction sufficiently fast for practical use, a catalyst such as a common stainless steal SUS316 can be introduced.

4. Conclusions

We have succeeded in establishing the kinetics and the equilibrium of the decomposition of formic acid, the WGS reaction intermediate, on the basis of the NMR spectroscopic analysis of the reactant and products. First the catalytic effect of acid on the decarbonylation is quantitatively analyzed, and it is found that the decarbonylation rate is first-order with respect to the concentration of formic acid and the proton, respectively. The equilibrium of the decarbonylation has been investigated under strongly acidic conditions where the competitive decarboxylation is negligibly slow. In determining the equilibrium constant of the decarbonylation, we have formulated the effect of the filling factor (the ratio of the liquid-phase volume to the total reactor volume) on the product yield. The equilibrium constant of the decarbonylation varies from 0.15 to 4.2 as the temperature rises from 170 to 280 °C on the liquid branch of the saturation curve, and this indicates that the decarbonylation can be controlled either to the formic acid side or to the CO side depending on the temperature and the filling factor. The low temperature and the high filling factor shift the equilibrium to the formic acid side. As for the decarboxylation path, the pH dependence of the reaction rate suggests that the decarboxylation consists of acid-induced and water-induced pathways, where the former is dominant in acidic conditions and the latter in basic conditions. The difference in the pH dependence

between the decarbonylation and the decarboxylation makes it possible to kinetically control the decomposition product of formic acid by the pH of the solution; the decarbonylation is dominant in acidic conditions, while the decarboxylation is dominant in basic conditions.

The detailed knowledge of the decarbonylation and the decarboxylation has provided a scheme for controlling the water-gas-shift reaction. We have proposed two examples of application taking advantage of the existence of the reaction intermediate in the form of formic acid. One is the storage of hydrogen energy as formic acid. The reaction conditions ideal for the conversion of CO into formic acid are (i) a relatively low temperature of ~200 °C, (ii) addition of such a strong acid as HCl, and (iii) a high filling factor. The other possible application is the fixation of CO_2 as formic acid through the reverse decarboxylation in basic conditions.

Acknowledgment. This work is supported by a Grant-in-Aid for Scientific Research (Nos. 15205004 and 18350004) from Japan Society for the Promotion of Science, by a Grant-in-Aid for Scientific Research on Priority Areas (No. 15076205) and a Grant-in-Aid for Creative Scientific Research (No. 13NP0201) from the Ministry of Education, Culture, Sports, Science, and Technology, and by ENEOS Hydrogen Trust Fund.

References and Notes

(1) Tsujino, Y.; Wakai, C.; Matubayasi, N.; Nakahara, M. *High-Pressure Sci. Technol.* **1999**, *9*, 66.

(2) Yu, J.; Savage, P. E. *Ind. Eng. Chem. Res.* **1998**, *37*, 2.

(3) Bjerre, A. B.; Sorensen, E. *Ind. Eng. Chem. Res.* **1992**, *31*, 1574.

(4) Maiella, P. G.; Brill, T. B. *J. Phys. Chem. A* **1998**, *102*, 5886.

(5) Bröll, D.; Kaul, C.; Krämer, A.; Richter, T.; Jung, M.; Vogel, H.; Zehner, P. *Angew. Chem., Int Ed.* **1999**, *38*, 2998−3014.

(6) Wakai, C.; Yoshida, K.; Tsujino, Y.; Matubayasi, N.; Nakahara, M. *Chem. Lett.* **2004**, *33*, 572.

(7) Yoshida, K.; Wakai, C.; Matubayasi, N.; Nakahara, M. *J. Phys. Chem. A* **2004**, *108*, 7479.

(8) Matubayasi, N.; Nakahara, M. *J. Chem. Phys.* **2005**, *122*, 074509.

(9) Melius, C. F.; Beergan, N. E.; Shepherd, J. E. *Symp. (Int.) Combust./ Combust. Inst., 23rd* **1990**, 217−223.

(10) Akiya, N.; Savage, P. E. *AIChE J.* **1998**, *44*, 405−415.

(11) Yagasaki, T.; Saito, S.; Ohmine, I. *J. Chem. Phys.* **2003**, *118*, 2446.

(12) Kroschwitz, J. I. *Encyclopedia of Chemical Technology*, 4th ed.; Wiley: New York, 1991.

(13) McCollom, T. M.; Seewald, J. S. *Geochim. Cosmochim. Acta* **2003**, *67*, 3625.

(14) Morooka, S.; Wakai, C.; Matubayasi, N.; Nakahara, M. *J. Phys. Chem. A* **2005**, *109*, 6610.

(15) Nagai, Y.; Morooka, S.; Matubayasi, N.; Nakahara, M. *J. Phys. Chem. A* **2004**, *108*, 11635.

(16) Release on the IAPWS Formulation 1995 for the Thermodynamic Properties of Ordinary Water Subtances for General and Scientific Use.

(17) If the decoupling is not performed, the ^{13}C peak corresponding to $H^{13}COOH$ has a line shape far from Lorentzian and is not suitable for quantitative analysis.

(18) Fernández-Prini, R.; Alvarez, J. L.; Harvey, A. H. *J. Phys. Chem. Ref. Data* **2003**, *32*, 903.

(19) The amount of CO produced by the decomposition of HCOONa at 1 mol kg^{-1} and 240 °C for 300 h was below the detection limit of 0.01 mol kg^{-1}. This means that the decarbonylation rate of HCOONa is not larger than 10^{-8} mol kg^{-1} s^{-1}, which is 10^4 times as small as that of HCOOH with 0.10 mol kg^{-1} HCl. The concentrations of the proton and the neutral formic acid HCOOH in eq 8 can be estimated from the dissociation constant of formic acid presented in section 3.3; $[H^+] = \sim 10^{-8}$ mol $kg^{-1}$and $[HCOOH] = 10^{-5}$ mol kg^{-1}. Thus eq 8 is consistent with the slow decarbonylation rate observed for HCOONa.

(20) Blake, P. G.; Hinshelwood, C. *Proc. R. Soc. London, Ser. A* **1960**, *255*, 444.

(21) Takahashi, H.; Hisaoka, S.; Nitta, T. *Chem. Phys. Lett.* **2002**, *363*, 80.

(22) Hori, T.; Takahashi, H.; Nitta, T. *J. Comput. Chem.* **2003**, *24* (2, Jan 30), 209−221.

(23) In hydrothermal conditions, the undissociated form of the water molecule often plays an active role in determining the reaction pathway. Indeed, it was demonstrated experimentally that the reaction proceeds without acid or base in a practical time scale for ether and C1 chemical reaction.[14,15] Correspondingly, several theoretical works investigated the role of the undissociated form of water in sub- and supercritical water reactions, and proposed concerted mechanisms which are not catalyzed by acid or base.[9−11,21] In the present work, however, the reaction pathway does not correspond to the one suggested by Yagasaki et al.[11] As shown in the text, the reaction rate is proportional to the $[H^+]$ present in the system. The reaction pathway corresponding to the neutral, concerted transition state was not observed within our experimental time scale. The reaction solution (1 mol/kg HCOOH) is quite acidic (pH = 2−3) even in the absence of HCl, and the acid-induced path still overwhelms the neutral concerted path. This has been strongly supported by the observed rate order of 1.5 for the decarbonylation in the absence of HCl as shown in section 3.3. If the reaction is carried out in higher pH conditions and/or at higher temperatures where the acid dissociation is suppressed, then the neutral reaction path can be possible. It has not yet been theoretically done to compare the reaction mechanisms involving the formate ion and the proton.

(24) Reid, R. C.; Prausnitz, J. M.; Poling, B. E. *The properties of gases and liquids*, 4th ed.; McGraw-Hill: New York, 1987.

(25) Wagman, D. D.; et al. *J. Phys. Chem. Ref. Data* **1982**, *2*, Suppl. 2.

(26) Gurvich, L. V.; Veyts, I. V.; Alcock, C. B. *Thermodynamic Properties of Individual Substances Fourth Ed. Volume 1, O, H (D, T), F, Cl, Br, I, He, Ne, Ar, Kr, Xe, Rn, S, N, P and Their Compounds*; Hemisphere: Bristol, PA, 1989.

(27) Harned, H. S.; Owen, B. B. *The Physical Chemistry of Electrolyte Solutions*; Reinhold Publishing Corporation: New York, 1958.

(28) For the decarboxylation mechanism, the neutral, concerted pathway was suggested and theoretically studied by Yagasaki et al.[11] Based on this reaction mechanism, the rate law for the decarboxylation is modified from eq 26 to $v_{+2} = k'[HCOOH] + k''[HCOOH][OH^-]$, where k' and k'' are rate constants for the water-catalyzed and base-catalyzed paths, respectively. This rate law can be shown to be coincident with eq 26 by using the acid dissociation constant as follows: $v_{+2} = k'K_a^{-1}[HCOO^-][H^+] + k''K_a^{-1}K_w[HCOO^-]$, where K_w is the self-dissociation constant of water. This means that it is impossible to distinguish the reaction mechanisms experimentally. Theoretical studies including water and neutral formic acid have been carried out by Yagasaki et al.,[11] and now additional studies including ionic species (H^+, $HCOO^-$, and OH^-) are required.